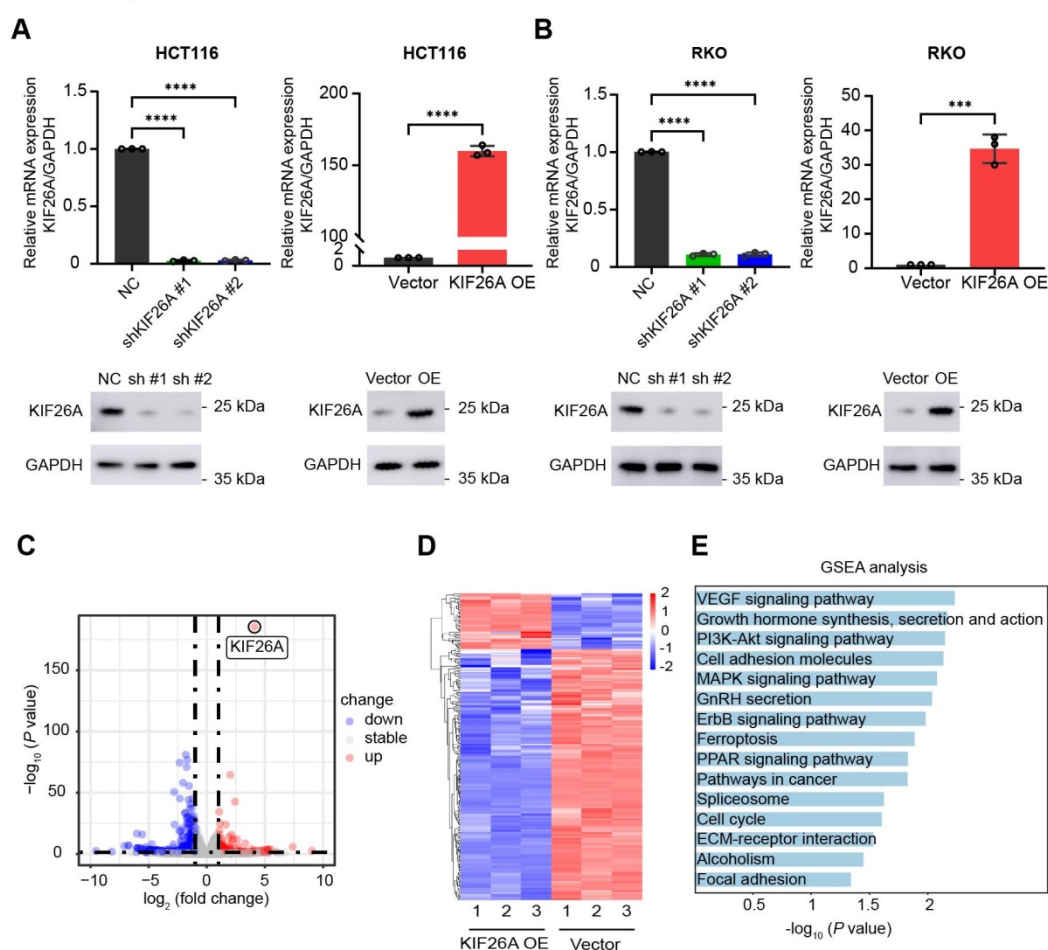


**Supplementary Material**  
**Supplementary Figures and Legends:**

Li et al, Figure S1



**Figure S1. KIF26A functions as a DNA damage response protein. Related to Figure 1.**

A. mRNA expression of KIF26A in KIF26A-sh and KIF26A-OE HCT116 quantified by RT-qPCR and Western blot (n = 3).

B. mRNA expression of KIF26A in KIF26A-sh and KIF26A-OE RKO quantified by RT-qPCR and Western blot (n = 3).

C-D. (C) Volcano plots and heatmap (D) showing genes upregulated (red, fold change > 2;  $P < 0.05$ ) or downregulated (blue, fold change < 0.5;  $P < 0.05$ ) in RKO cells overexpressing KIF26A.

Gene set enrichment analysis (GSEA) of differentially expressed genes showed several pathways, including the PI3K-AKT signaling pathway and cell adhesion molecules.

A and B, \*\*\* $P < 0.001$  or \*\*\*\* $P < 0.0001$ , determined by Student's *t*-test and one-way ANOVA;  $P$  value of less than 0.05 indicates a statistical difference. Error bars, mean  $\pm$  SD. A-B, three biological independent replicates were performed.

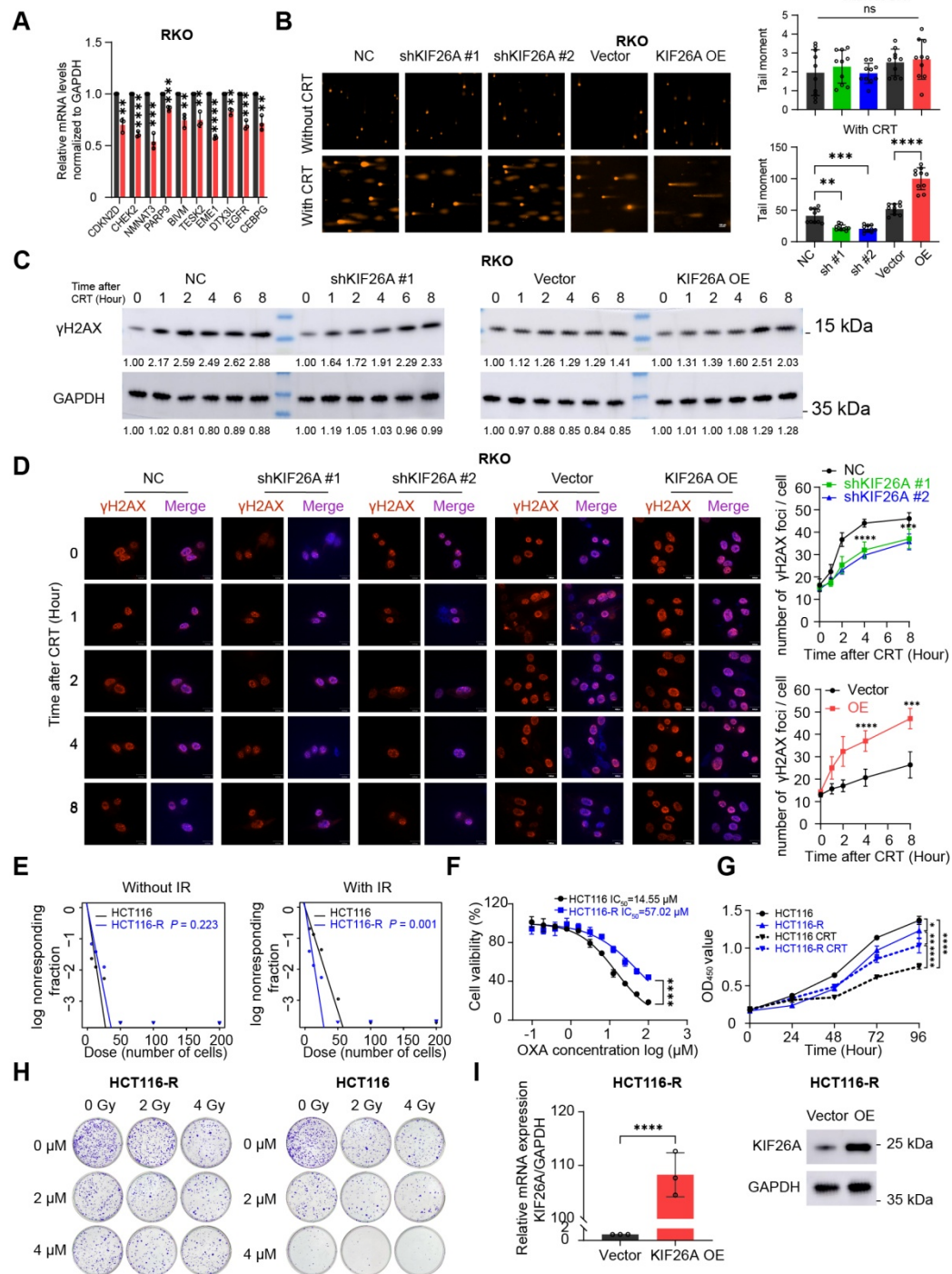


**Figure S2. KIF26A inhibits DNA damage repair. Related to Figure 2.**

- A. Verification of the expression changes of the differentially expressed genes in the DNA repair pathway in RKO cell (n = 3).
- B. DNA damage in KIF26A-modulated RKO cells after CRT was assayed by comet assay (n = 10). Scale bars, 100  $\mu$ m.
- C, D. DNA double-strand breaks expressed by  $\gamma$ -H2AX level in KIF26A knockdown or overexpressing RKO cells treated with or without CRT. (C) Shows  $\gamma$ -H2AX by western blot analysis. (D) Shows images of  $\gamma$ -H2AX foci in cells at various time

points of IR as indicated (n = 3). Scale bars, 10  $\mu$ m.

- E. Cell survival fractions via extreme limiting dilution analysis in HCT116 parental cells (HCT116) and HCT116 chemoradiotherapy-resistant cells (HCT116-R) with or without IR (4 Gy).
- F. IC<sub>50</sub> values of Oxaliplatin(OXA)in HCT116 parental cells (HCT116) and HCT116 chemoradiotherapy-resistant cells (HCT116-R) (n = 6).
- G. CCK8 assay showed the proliferation ability of HCT116 parental cells (HCT116) and HCT116 chemoradiotherapy-resistant cells (HCT116-R) (n = 6). CRT group treated with radiation (4 Gy) and chemotherapy (1  $\mu$ g/mL of Oxaliplatin); Control group treated with the same volume of DMSO as the CRT group and without radiation.
- H. The colony formation assay showed the proliferation ability of HCT116 parental cells (HCT116) and HCT116 chemoradiotherapy-resistant cells (HCT116-R) under different doses of radiotherapy and chemotherapy drugs (n = 3).
- I. mRNA expression of KIF26A in KIF26A-OE HCT116-R quantified by RT-qPCR and Western blot (n = 3).

A, B, D, F, G, I, \* $P < 0.05$ , \*\* $P < 0.01$ , \*\*\* $P < 0.001$  or \*\*\*\* $P < 0.0001$ , A, E, F, I, determined by Student's *t*-test; B, D, G, determined by one-way ANOVA. *P* value of less than 0.05 indicates a statistical difference. Error bars, mean  $\pm$  SD. For all panels, three biological independent replicates were performed.

Li et al, Figure S3

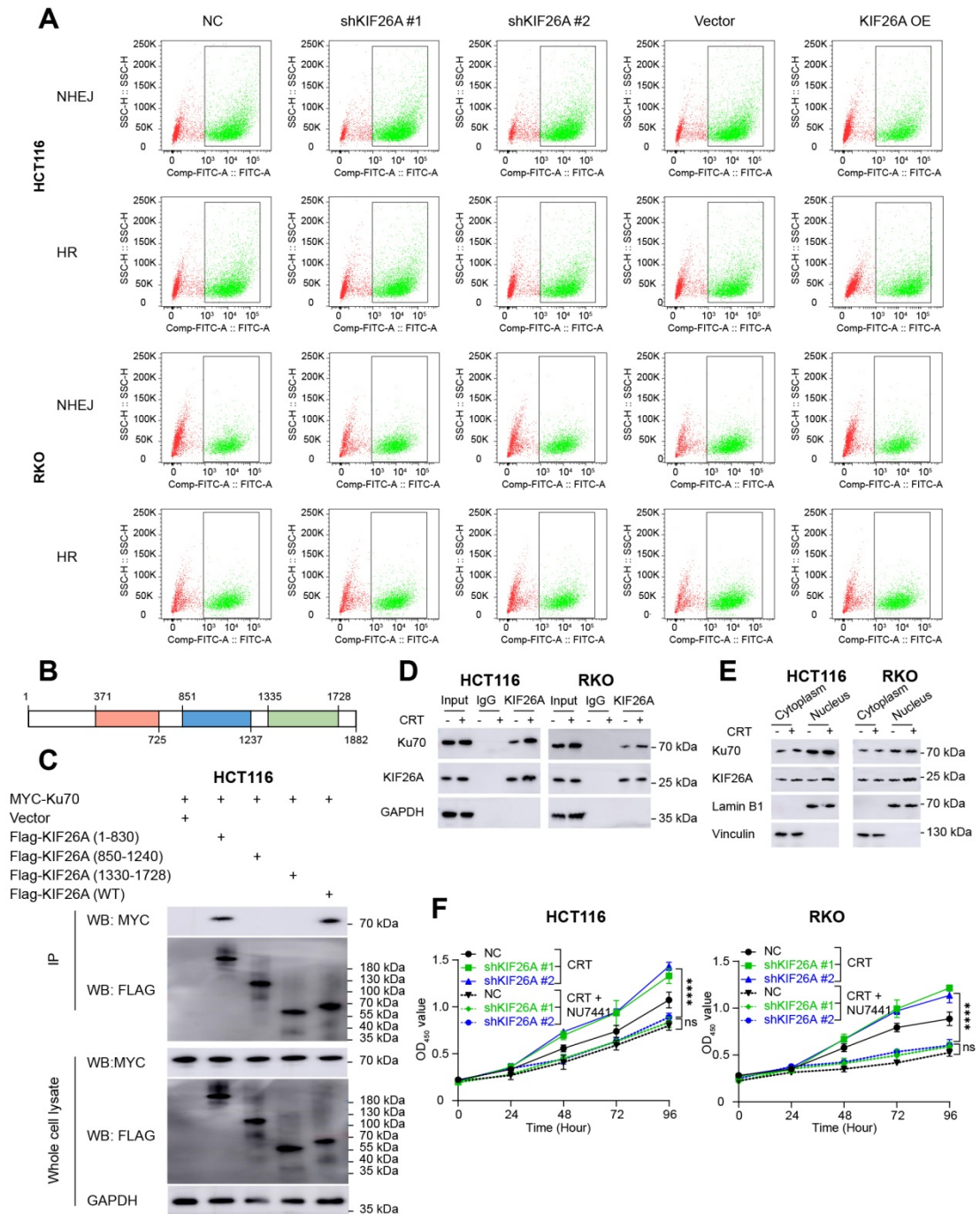


**Figure S3. KIF26A inhibits the NHEJ repair pathway by binding to Ku70. Related to Figure 3.**

**A.** Flow cytometry analysis of KIF26A knockdown or overexpression effects on NHEJ and HR pathways. HCT116 and RKO cells were transfected with pEJ5-GFP or DR-GFP. After 24 h, cells were transfected with I-SceI. GFP expression was quantified by flow cytometry 24 hours later, with example gating.

**B.** Analysis of the architecture of KIF26A.

- C. Immunoblot analysis of Myc-tagged Ku70 co-immunoprecipitated with FLAG-tagged full-length (WT) KIF26A and its truncated variants.
- D. In HCT116 and RKO cells, Western blot probed KIF26A and Ku70 proteins immunoprecipitated via anti-KIF26A antibody, with IgG as the control.
- E. Analysis of KIF26A and Ku70 levels in cytoplasmic and nuclear fractions of HCT116 cells by Western blot.
- F. CCK8 assay showed the proliferation ability of HCT116 and RKO control (NC) and KIF26A-knockdown (sh) cells following CRT treatment with or without NU7441 (n = 6).

A, C-E three independent replicates were performed. CRT group treated with radiation (8 Gy) and chemotherapy (2  $\mu\text{g}/\text{mL}$  of Oxaliplatin). F. Combination groups were treated with NU7441 (1  $\mu\text{M}$ ) for 2 hours prior to CRT treatment. A and C-F, three biological independent replicates were performed.

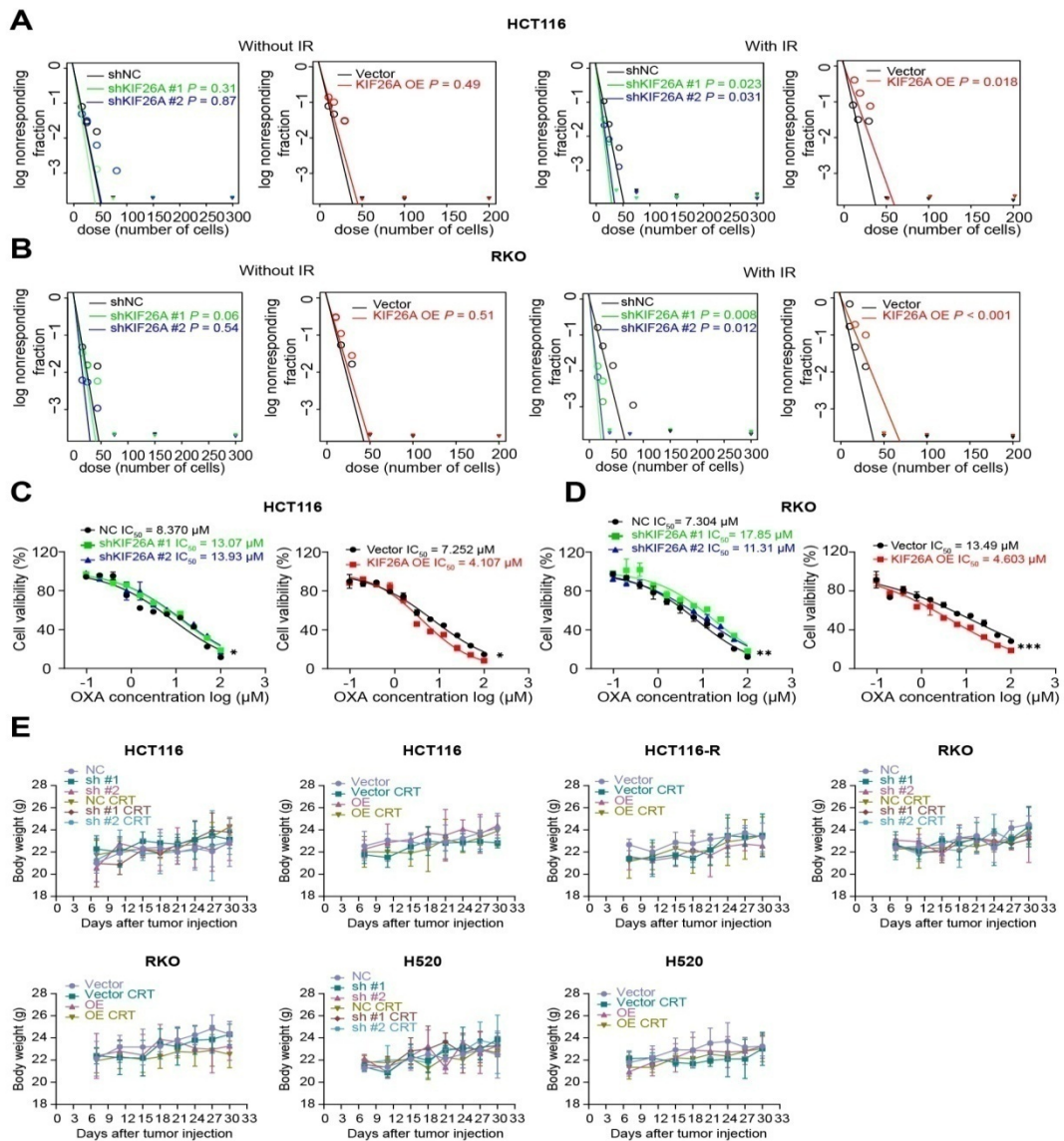


**Figure S4. KIF26A increases chemoradiotherapy sensitivity. Related to Figure 4.**

A-B. Cell survival fractions via extreme limiting dilution analysis in KIF26A-knockdown and KIF26A-OE HCT116 (A) and RKO (B) cells with or without IR (4 Gy).

C-D.  $IC_{50}$  values of Oxaliplatin (OXA) in KIF26A-knockdown and KIF26A-OE HCT116 (C) and RKO (D) cells ( $n = 6$ ).

E. In vivo toxicity monitoring. Bodyweight growth curves of control and KIF26A-knockdown or KIF26A-overexpression tumors in HCT116, HCT116-R, RKO and H520 cells with or without CRT treatment ( $n = 4-5$  per group).

A-D,  $*P < 0.05$ ,  $**P < 0.01$ ,  $***P < 0.001$ , A-D, determined by Student's  $t$ -test and one-way ANOVA.  $P$  value of less than 0.05 indicates a statistical difference. Error bars, mean  $\pm$  SD. For all panels, three biological independent replicates were performed.

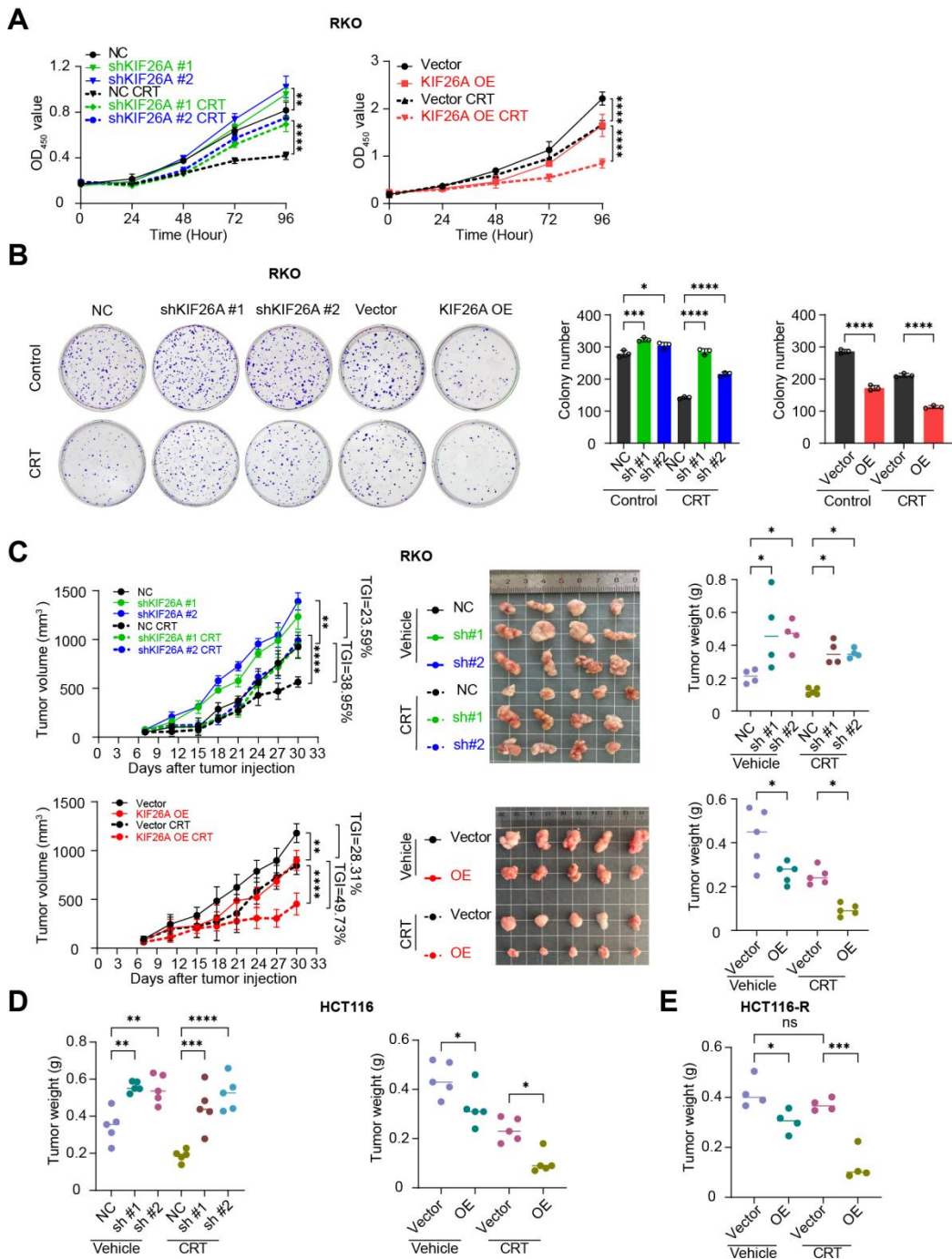


**Figure S5. KIF26A increases chemoradiotherapy sensitivity. Related to Figure 4.**

A. CCK8 assay showed the proliferation ability of RKO cells following KIF26A knockdown or overexpression (n = 6).

B. The colony formation assay showed the proliferation ability of RKO cells following KIF26A knockdown or overexpression (n = 3).

C. RKO cells were subcutaneously injected into NSG mice and then treated with radiation (4 Gy) and Oxaliplatin (5 mg/kg) or not at the indicated time points (n = 4-5 per group). Tumor growth curves (left), excised tumor images (middle) and

tumor weight (right) of control and KIF26A-knockdown tumors, KIF26A-overexpression tumors in RKO cells with or without CRT treatment (n = 5 per group). TGI, percentage of tumor growth inhibition.

D. Tumor weight of control and KIF26A-knockdown tumors, KIF26A-overexpression tumors in HCT116 cells.

E. Tumor weight of control and KIF26A-overexpression tumors in HCT116-R cells.

A and B, CRT group treated with radiation (4 Gy) and chemotherapy (1  $\mu\text{g}/\text{mL}$  of Oxaliplatin); Control group treated with the same volume of DMSO as the CRT group and without radiation. A-C,  $**P < 0.01$ ,  $***P < 0.001$  and  $****P < 0.0001$ ; determined Student's *t*-test and one-way ANOVA; *P* value of less than 0.05 indicates a statistical difference. Error bars, mean  $\pm$  SD. A and B, three biological independent replicates were performed.

Li et al, Figure S6

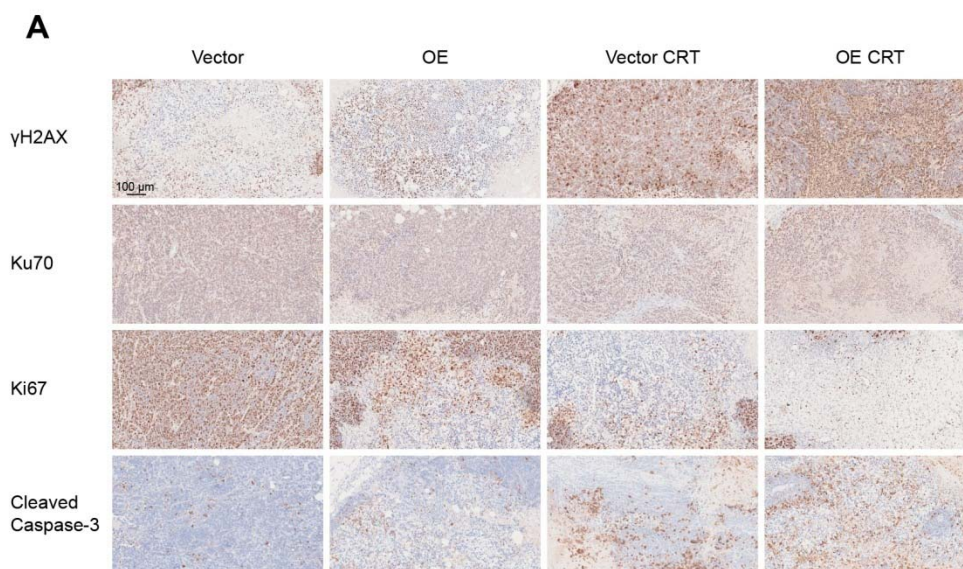


**Figure S6. Immunohistochemistry of HCT116 xenografts. Related to Figure 4.**

A. Staining for  $\gamma$ -H2AX, Cleaved Caspase-3, KU70, and Ki67 in tumors. Scale bar: 100  $\mu\text{m}$ . Three independent biological replicates were performed.

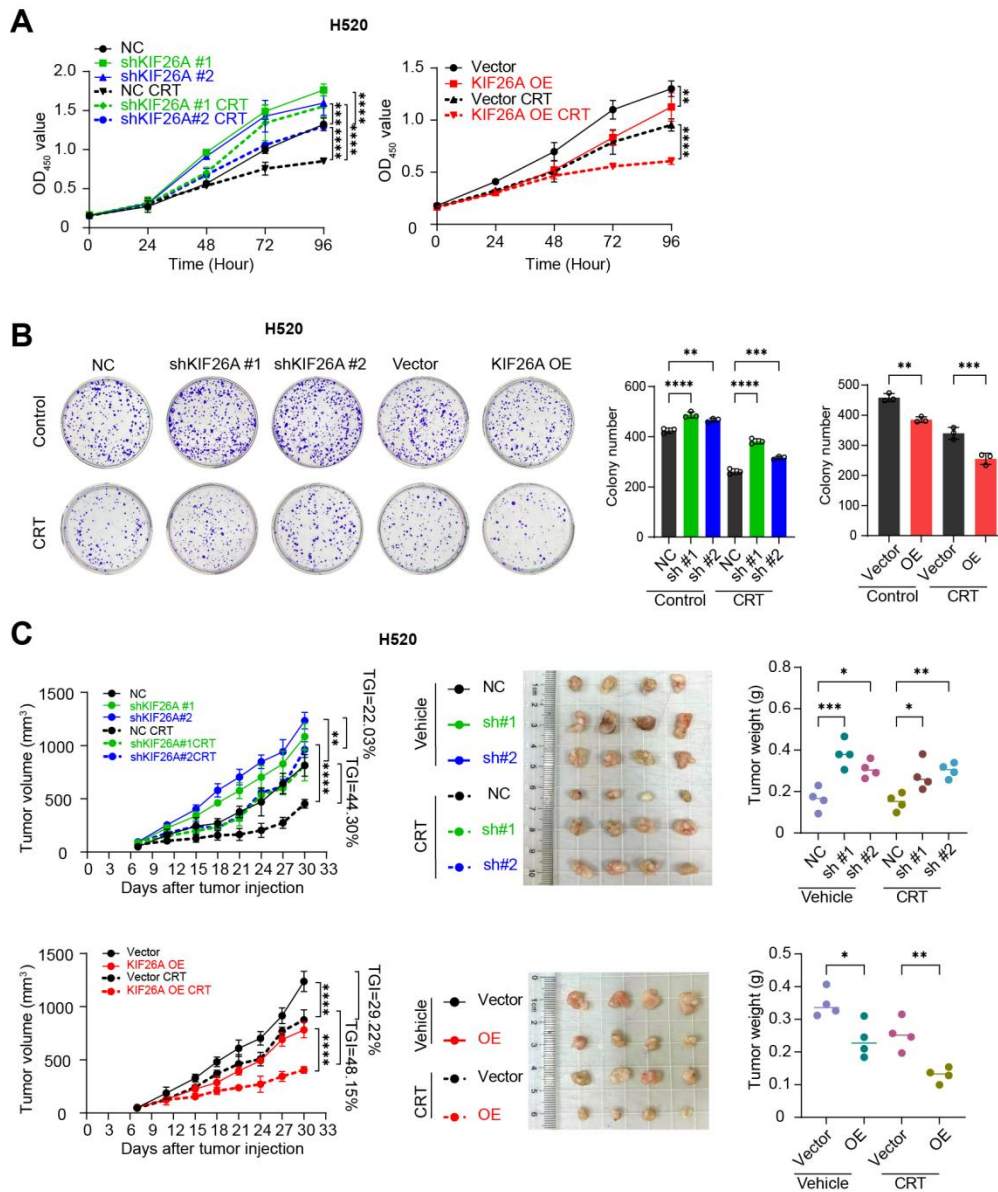


**Figure S7. KIF26A increases chemoradiotherapy sensitivity. Related to Figure 4.**

A. CCK8 assay showed the proliferation ability of H520 cells following KIF26A knockdown or overexpression (n = 6).

B. The colony formation assay showed the proliferation ability of H520 cells following KIF26A knockdown or overexpression (n = 3).

C. H520 cells were subcutaneously injected into NSG mice and then treated with radiation (4 Gy) and Oxaliplatin (5 mg/kg) or not at the indicated time points (n = 4 per group). Tumor growth curves (left), excised tumor images (middle) and

tumor weight (right) of control and KIF26A-knockdown tumors, KIF26A-overexpression tumors in H520 cells with or without CRT treatment (n = 4 per group). TGI, percentage of tumor growth inhibition.

A and B, CRT group treated with radiation (4 Gy) and chemotherapy (1  $\mu\text{g}/\text{mL}$  of Oxaliplatin); Control group treated with the same volume of DMSO as the CRT group and without radiation. A-C,  $**P < 0.01$ ,  $***P < 0.001$  and  $****P < 0.0001$ ; determined Student's *t*-test and one-way ANOVA; *P* value of less than 0.05 indicates a statistical difference. Error bars, mean  $\pm$  SD. A and B, three biological independent replicates were performed.

Li et al, Figure S8

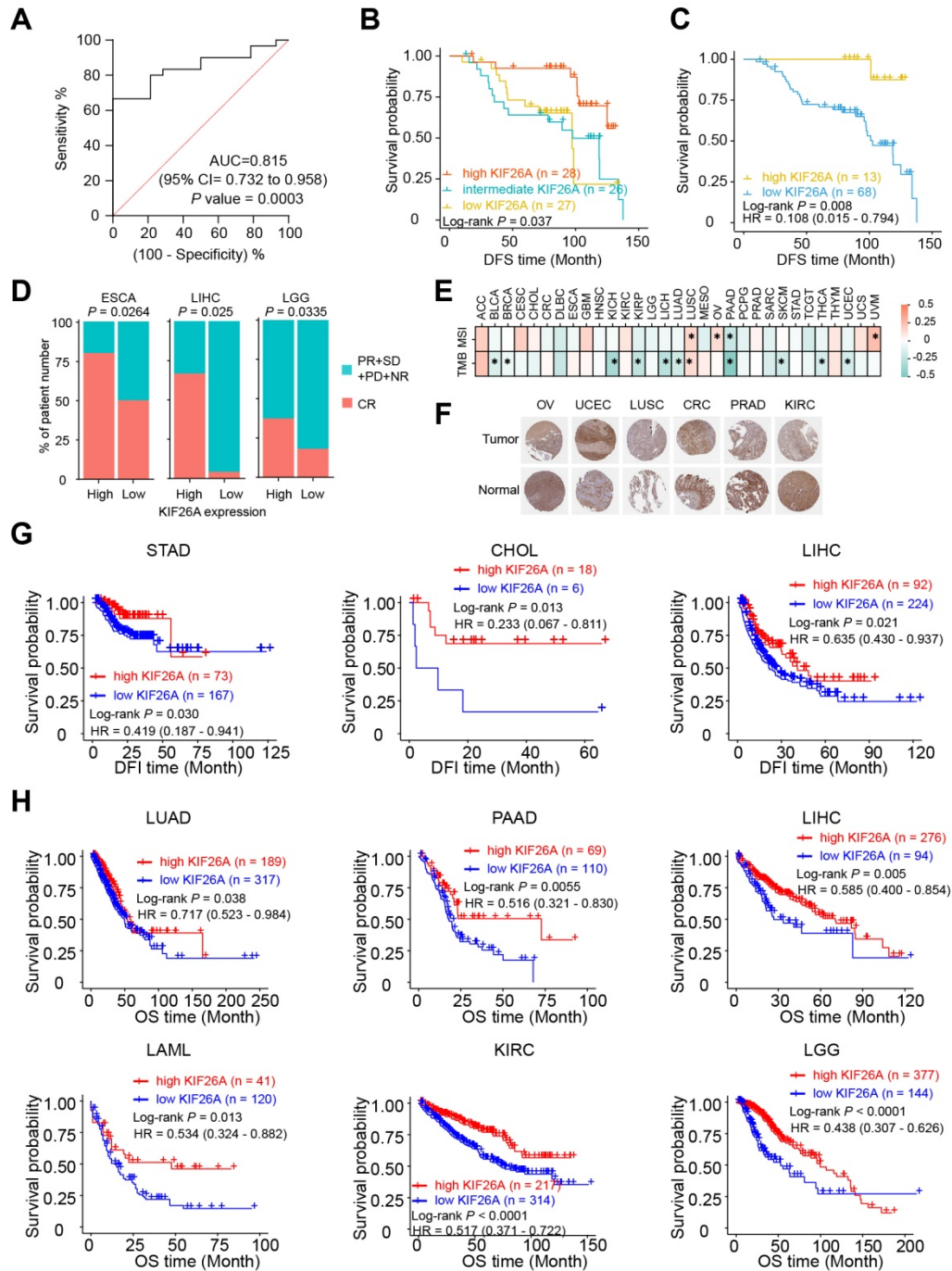


**Figure S8. Reduced KIF26A expression informs poor prognosis of patients to chemoradiotherapy. Related to Figure 7.**

A. Receiver operating characteristic (ROC) curve for evaluating the prognostic performance of KIF26A expression. The optimal cutoff value (7.44) was determined by maximizing the Youden index.

B. Kaplan-Meier survival curves based on tertile stratification of KIF26A expression. Patients were divided into low, intermediate and high expression groups of equal size.

- C. Kaplan-Meier survival curves based on the optimal ROC-determined cutoff for KIF26A expression. Patients were stratified into low- and high-expression groups using this cutoff.
- D. The correlation between KIF26A expression and the response of CRC patients to chemotherapy and radiotherapy. The left panel represents analysis of the TCGA-ESCA dataset (n = 58). The middle panel represents analysis of the TCGA-LIHC dataset (n = 27). The right panel represents analysis of the TCGA-LGG dataset (n = 217)(NR, no response; PD, progressive disease; SD, stable disease; PR, partial response; CR, complete response).
- E. Correlation analysis between KIF26A expression and genomic instability markers using the TCGA pan-cancer dataset in patients receiving chemotherapy or radiotherapy or both.
- F. Immunohistochemistry of cancer and normal tissues from the Human Protein Atlas.
- G. Kaplan-Meier analyses of disease-free interval (DFI) using the TCGA pan-cancer dataset in patients receiving chemotherapy or radiotherapy or both, based on KIF26A expression levels. The TCGA cancer acronyms are listed in the Abbreviations section.
- H. Kaplan-Meier analyses of overall survival (OS) using the TCGA pan-cancer dataset in patients receiving chemotherapy or radiotherapy or both, based on KIF26A expression levels.